

Article

Influence of Multivector Field on Paste Preparation and Formation of Negative Electrodes of Lead Batteries

Boris Shirov ^{1,*} , Vesselin Naidenov ¹ and Urie Markov ²

¹ Institute of Electrochemistry and Energy Systems, Lead–Acid Batteries Department, Bulgarian Academy of Sciences, Acad. Georgi Bonchev Str., Bl. 10, 1113 Sofia, Bulgaria; v_naid@abv.bg

² TASC Ltd., 1000 Sofia, Bulgaria; office@tasc.bg

* Correspondence: boris.shirov@iees.bas.bg

Abstract: During the operation of the negative electrode, some critical processes take place, which are limiting factors for the operation of lead–acid batteries. To improve the efficiency of the negative active material and minimize these processes, external application of multivector field is proposed. Two applications of the multivector field are studied: during negative paste preparation and during formation. It is established that, when applying multivector field during negative paste preparation, the chemical processes proceed more efficiently. The results are better phase composition and crystallinity of the cured paste, thus increasing the capacity of the consequently built lead batteries by 12% on average. The application of a multivector field during the formation of negative active materials in lead batteries has a positive effect on the skeletal structure, the size and shape of the Pb crystals. This ensures longer service life, which is confirmed by the 17.5% Depth of Discharge continuous tests on 12 V/75 Ah batteries. The batteries formed under the influence of external multivector field showed 20% longer cycle life. Based on the experimental result, a most probable mechanism of the influence of the multivector field on the chemical and electrochemical processes in lead batteries during negative paste preparation and formation of negative active masses is proposed.

Keywords: lead–acid battery; formation process; negative active material; paste electrode; magnetic field



Citation: Shirov, B.; Naidenov, V.; Markov, U. Influence of Multivector Field on Paste Preparation and Formation of Negative Electrodes of Lead Batteries. *Batteries* **2021**, *7*, 24. <https://doi.org/10.3390/batteries7020024>

Academic Editor: Catia Arbizzani

Received: 28 February 2021

Accepted: 30 March 2021

Published: 9 April 2021

Publisher's Note: MDPI stays neutral with regard to jurisdictional claims in published maps and institutional affiliations.



Copyright: © 2021 by the authors. Licensee MDPI, Basel, Switzerland. This article is an open access article distributed under the terms and conditions of the Creative Commons Attribution (CC BY) license (<https://creativecommons.org/licenses/by/4.0/>).

1. Introduction

The constant increase in human energy needs together with the continuous depletion of natural energy resources over the last several decades bring forward the important issues of rational and effective use, storage and processing of energy. This, in turn, sets a number of important and challenging tasks for scientists and engineers, especially the tasks to invent new energy sources and improve existing ones.

Nowadays, we are witnessing a continuous expansion of the application fields of lead batteries. Lead batteries are used to power almost every type of motor vehicle, aircraft and watercraft; they are used in the energy industry for electrical power storage in all types of renewable energy sources, including photovoltaic, wind power and ocean power, as well as for buffer systems in nuclear and hydro power plants [1].

Furthermore, lead batteries are used as backup power supply systems for different commercial installations such as computer systems in the banking sector, telecom base-stations and life-supporting medical equipment.

This wide application of lead batteries naturally leads to ever increasing requirements for lead battery quality with regard to operating, ergonomic and ecological parameters.

Lead–acid battery technology is one of the oldest technologies for accumulating electrical energy; however, the research into making lead batteries more competitive compared to newer battery chemistries is ongoing. The low cost makes lead–acid batteries commercially significant, but its main limitations are considered to be the low dynamic charge acceptance, as well as limited specific energy [2]. To address these issues, many

additives to the negative and the positive electrodes have been proposed [3,4]. In addition, additives to the electrolyte [5] are considered as prospective for improving the performance of lead-batteries. The use of additives in the active materials or the electrolyte has been fairly well studied in the literature, but there is limited data for the application of external radiation which exert an influence on the chemical and electrochemical processes that take place in the lead battery.

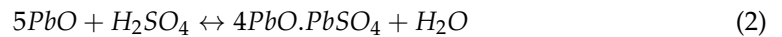
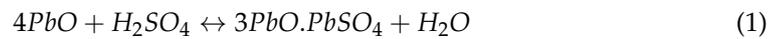
The main factors that lead to a decrease in the capacity of lead–acid batteries and shortening their service life are the change in the chemical composition and the crystal structure of the negative active mass [6–9]. The aim of the present work is to study the possibility of reducing the adverse electrochemical processes that are responsible for these effects through the application of external multivector field. Since all chemical substances are characterized by their own magnetic moments [10], the application of such a field should affect this specific parameter. The multivector field influences the chemical and electrochemical processes on the negative electrodes of lead–acid batteries. As a result, a controlled effect on the construction of the chemical compositions and crystal structures of the negative active mass is achieved. The new crystal structures subsequently affect the reactivity of the substances involved in the processes of charge and discharge. Two applications of the multivector field are studied during negative paste preparation and formation. The multivector field is composed of two components, a strong constant magnetic field in combination with variable electromagnetic radiation with characteristics corresponding to the processes occurring on the negative electrode.

As mentioned earlier, there are limited data in the literature on the usage of external influences on the processes during paste preparation and formation of lead–acid batteries. V. Naidenov and U. Markov [11] described how the application of ultrasonic waves influence the formation of lead batteries. They studied in detail how this radiation affects the formation processes and the structure of the formed active masses. It was found that ultrasonic waves applied during formation increase the content of PbO_2 in the positive active mass, thus improving the cycle life and the capacity performance of batteries formed under the influence of such radiation. The authors also concluded that the rate of the electrochemical reactions on the negative active mass is not influenced by the application of ultrasonic waves during the formation process.

In their research, Khare and collaborators [12] propose a novel magnetic field probing technique for determination of the state of health of lead batteries. They used an AC magnetic field as a noninvasive tool during battery cycling. They observed the battery performance under magnetic field during battery cycling and found that the direction of the magnetic field in respect to the battery plates is essential. If the magnetic field flux lines are parallel to the plates of the lead acid battery, the strength of the magnetic field increases; if they are perpendicular, the plates screen most of the flux lines. In two papers, Battaglia and Newman [13,14] studied the theory of the magnetic field effects in high-power batteries, giving the first approximation to the instantaneous current distribution in bipolar lead–acid batteries. Another novel application of magnetic field in studying lead–acid batteries is proposed by Harrison et al. [15,16]. These researchers used the methods of magnetic tomography to non-invasively measure the current distribution of experimental lead cells. However, most of the reported external methods are intended to measure the performance parameters of lead–acid batteries, rather than to influence the chemical and electrochemical processes in them.

The main chemical processes involved in the preparation of pastes for active materials for lead–acid batteries are described by Barnes and Mathieson [17]. The processes are further studied by D. Pavlov [18]. The main components of the paste are basic lead sulfates, non-reacted and hydrated lead oxides, free metallic lead particles and basic lead carbonates. During paste preparation, water and sulfuric acid are added to leady oxide powder. As a result, tribasic lead sulfate $3\text{PbO}\cdot\text{PbSO}_4\cdot\text{H}_2\text{O}$ (3BS) and tetrabasic lead sulfate $4\text{PbO}\cdot\text{PbSO}_4$

(4BS) particles are formed. The main reactions during paste mixing for preparation of 3BS and 4BS pastes are described by the following equations.

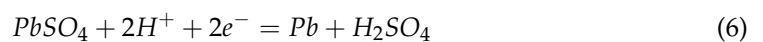
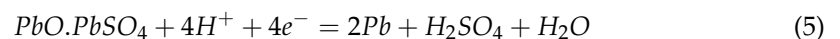
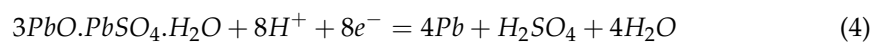


The chemical nature of the lead sulfate formed in the paste during its preparation is important since it affects the efficiency of the consequent processes of plate formation, its electrochemical performance and its durability under discharge/charge cycling. 3BS pastes are most commonly used by the industry for the production of positive and negative plates [18].

4BS is much more difficult to form, particularly in sulfuric acid solutions of concentrations greater than 15%, but it contributes to the formation of a strong and stable morphology in the crystal structure of the plate. In battery types where 4BS is preferred, it is more common to obtain it during the curing process rather than during paste mixing.

When applying a multivector field with specifically calculated parameters during the preparation of negative pastes, 3BS with improved quality and morphology is obtained. The application of the multivector magnetic field continues during the entire paste preparation process.

It has been shown in several papers that the process of formation of the negative active material occurs in two stages [18–20]. During the first stage, 3BS and PbO, after reduction, form the lead skeleton of the negative active mass responsible for the mechanical bonding and adhering of the active mass to the plates. During the second stage of the formation process, due to the reduction of the lead sulphates, small lead crystals with a large surface area are formed. It is mainly on these latter crystals that the capacity of the negative active mass depends. The reactions that occur during the formation of the negative active mass are as follows:



When a multivector field, with pre-defined parameters for formation, is applied during the first stage of formation of the electrodes, it creates conditions for more effective electrochemical and crystallization processes to occur, thus ensuring uniform formation of the plates. The multivector field exerts an influence on the mobility of the H⁺ ions, which affects the overall rate and efficiency of the formation processes. Formed batteries with the application of multivector field have improved performance characteristics such as better charge acceptance, higher capacity and extended service life.

As it was mentioned above, there are only few publications that present results of application of external radiation during the paste mixing or formation processes. In the literature, there are publications on the use of ultrasonic waves [11,21] during the formation of the active materials. So far, there are no available publications on using a combination of constant magnetic field and electromagnetic radiation.

The purpose of this paper is to show how application of a multivector field, applied during negative paste mixing, influences the phase composition and the crystalline structure. In addition, the effects of this field are investigated when applied during the process of formation of negative active mass of lead batteries, thus enhancing their operational parameters according to their application.

2. Materials and Methods

2.1. Multivector Field

For the purpose of this study, a special equipment for generating the multivector field was developed [22]. As mentioned earlier, the multi-vector field is composed of a strong constant magnetic field with specific density and direction of the magnetic flux. A variable electromagnetic field with characteristics corresponding to the processes occurring during the preparation and formation of the active masses for the lead–acid batteries is superimposed on this specific constant magnetic field.

The structures of arranged strong rare-earth neodymium magnets are used for the generation of the primary permanent magnetic field. High-grade neodymium magnets within the range N42–N52 are selected. The number and size of the high-grade neodymium magnets in the structure depends on the volume of the paste mixer or the physical size of the electrodes to be formed. Depending on the processes to be affected, the magnetic structure may be with unidirectional or multidirectional orientation with respect to the magnetic flux.

The superimposed electromagnetic field has variable characteristics corresponding to the processes that occur during paste preparation or the formation of the active masses for lead acid batteries. The field characteristics such as frequency, phase, amplitude and power are calculated on the basis of a mathematical model that takes into account the physical, chemical and electrochemical processes occurring during the paste preparation or active mass formation procedures. The device for emitting the multivector field consists of a magnetic structure of a linear configuration to generate the primary permanent magnetic field and a signal generator for the emission of the overlaying electromagnetic field.

For the experiments of this paper, a linear magnetic structure of 11 ring neodymium magnets with grade N42 was built. The ring magnets were put each facing the opposite polarity of the preceding magnet, i.e., north versus south versus north, and so on. On top of the linear magnetic structure, a coil was installed in order to act as an antenna for the superimposed electromagnetic field. The multivector field emitter showed on Figure 1 was then connected to a signal generator, patented by U. Markov [22], which is generating the overlaying electromagnetic field. Frequencies used were in the range of 40 kHz up to 100 kHz, with transmit power varying from 1 W up to 5 W, depending on whether the device is being used during the negative paste mixing or during the formation of lead batteries.

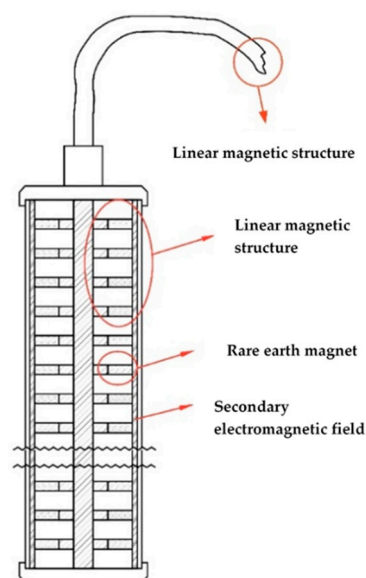


Figure 1. Multivector field emitter.

2.2. Negative Paste Preparation

The first part of this article describes the effects of the externally applied multivector magnetic field on the processes of negative paste preparation. During the past few years, many additives for enhancing the properties of the negative active material were researched, with carbon additives being in the main focus [3,23–25]. For the purpose of this paper, in order to assess the effects of the multivector field on the properties of the negative paste, a conventional negative active material recipe was used [26], which is presented on Table 1. Two negative electrode pastes were prepared: a control one prepared without the impact of a multivector field and the other one under the influence of a multi-vector magnetic field. The following formulation was used for the preparation of the negative pastes:

Table 1. Negative paste recipe.

Compound	Quantity
PbO	1000 g
Carbon black	4 g
BaSO ₄	8 g
Vanisperse A	2 g
H ₂ SO ₄ density 1.4 g/cm ³	75 mL
H ₂ O	110 mL

A mixer comprising a plastic cylindrical vessel and stainless-steel mechanical stirrers was used. When preparing the paste for the negative electrodes of lead–acid batteries, the lead oxide was first placed in the blender container. BaSO₄, Vanisperse A and Carbon black were then added and stirring of the dry mixture continued for two minutes. After homogenizing the mixture in the dry state, the required amount of distilled water was added and the stirring continued for three more minutes. Next, the sulfuric acid solution was added in portions of 20 mL and, finally, at the twentieth minute of the beginning of stirring, the last 35 mL solution of sulphuric acid was added. The total time of stirring of the paste from the starting moment of the addition of sulfuric acid solution was 30 min, the temperature of the prepared negative paste being continuously monitored to not exceed 40 °C.

When the negative electrode paste was prepared under the influence of a multivector field, the multivector field emitter was mounted on the side of the plastic cylindrical vessel. After stirring the mixture in the dry state, i.e., two minutes after the start of the procedure, the overlaying electromagnetic field was switched on. The field power was calculated based on the volume of the materials involved, but not exceeding 5 W per kilogram of paste. On completion of the paste preparation process, the multivector field emitter was switched off. The thus prepared pastes were pasted on grids with dimensions: height: 60 mm; width: 60 mm; thickness: 1.8 mm; weight: 21 g. Each plate was pasted with approximately 21 g of paste. All the pasted plates prepared with and without application of multivector field were cured together in a curing chamber under constant temperature and humidity control under the following conditions: 48 h at 35 °C and 98% relative humidity, followed by 24 h at 60 °C and 10% relative humidity. The cured negative plates were assembled in six 2 V/2.3 Ah lead–acid cells with AGM (Absorbed Glass Mat) separator—three control cells with negative electrode made with control paste and three with negative electrode made with a paste prepared under the influence of a multivector field. The positive electrodes of both groups of cells were standard positive electrodes. A cell design comprising two positive electrodes and one negative was chosen. The cells were filled with electrolyte of H₂SO₄ solution, with 1.25 g cm^{−3} specific gravity, soaked for 1 h and then were subjected to formation. The formation was performed by a standard formation program used in our studies in a water bath and the temperature was controlled not exceeding 40 °C. The formation factor was 1.5 times the theoretical nominal capacity, which corresponds to $Q_{\text{Form}1.5} = 6.9 \text{ Ah}$. After the formation of the two groups of cells, they were subjected to a 10-cycle capacity test. The capacity test was followed a standard C10 profile with

discharges conducted in a 10-h discharge mode with a current of 0.23 A to a final discharge voltage of 1.7 V. The charges were performed with 0.23 A current and an upper limit of the charging voltage of up to 2.58 V, the cells being recharged with 5% more capacity than the discharge capacity of the previous cycle.

All pastes and electrodes under testing were subjected to chemical analysis and X-ray diffraction analysis (XRD) immediately after the paste preparation was completed and after curing of the plates.

2.3. Negative Electrode Formation

The second part of this article investigates the effects of the externally applied multi-vector magnetic field on the negative electrode during formation. For the purpose of these tests, four 12 V/75 Ah unformed dry batteries were provided by a battery manufacturer. The unformed batteries used for the study were produced with seven positive electrodes and six negative electrodes per cell and were selected from one production batch of equal weight. The formation procedure and formation current profile employed were as per the battery manufacturer's specification, which is shown in Table 2. A water-based H₂SO₄ solution with 1.25 g/cm³ density was used as electrolyte for the formation process and the same amount of electrolyte was poured in each battery cell. At the beginning of the formation process, all batteries were flooded with electrolyte and were left to soak for 1 h. After that the batteries were divided into two groups: the first one comprised two batteries formed under the external influence of a multivector field and the second one comprised control batteries formed without application of multivector field. During the formation process, the temperature in the water bath was maintained below 40 °C. The parameters of the formation profile used are given in the following table.

Table 2. Formation profile.

Step Number	Mode	Current, A	Duration, h
1	Charge	2	0.25
2	Charge	20	7
3	Pause	0	0.25
4	Charge	19	6
5	Pause	0	0.25
6	Charge	17	6

For the first group of batteries, a multivector field emitter was mounted next to each battery. The overlaying electromagnetic field was switched on after the first step of the formation profile and was switched off at the end of the formation process. The field power was calculated according to the design of the battery and the volume and weight of the materials used for the negative active masses.

On completion of the formation process, two batteries of each group were torn down for analysis of the negative electrodes by different methods, including chemical analysis, X-ray diffraction analysis, Brunauer–Emmett–Teller (BET) surface area analysis and scanning electron microscopy (SEM). The remaining two batteries were subjected to cycling tests down to 17.5% depth of discharge (DoD), as per VW 75073: 2012-07 standard specification. The batteries were put in a water bath at 27 °C. Then, they were discharged for 2.5 h with a current of 15 A. Further cycling continued employing the following program: charge with 26.25 A for 40 min with voltage limited to 14.4 V followed by discharge for 30 min with 26.25 A. The end-of-life criterion was when the discharge voltage during cycling fell down below 10 V. The end of discharge voltage was recorded at every cycle. The discharge voltage and the total number of cycles completed by the batteries under test were used to assess the effects of the multivector field applied during formation of the batteries on their cycle life performance.

3. Results and Discussions

3.1. Application of Multivector Field during Negative Paste Preparation

As mentioned earlier, two negative pastes were prepared, one with external application of multivector field and one without external influence. We will use the abbreviation MVFP (MultiVector Field Paste) for the negative paste prepared with external emission and for the other we shall use CP (Control Paste) for the remainder of this paper. The concentrations of Pb, PbSO₄ and PbO in the pastes were determined by volumetric titration, with a KMnO₄ solution and gravimetric precipitation with 5% BaCl₂. Analytical grade reagents and bi-distilled water were used for all solutions.

Table 3 summarizes the results of the chemical analysis of the prepared negative pastes before curing. The PbSO₄ content in the CP is lower by 4.23% than in the MVFP. When comparing the content of Pb and PbO in the two pastes, the CP paste contains 1.3% more Pb than the MVFP paste, while the content of PbO is 2.71% less than in the CP. During the chemical analysis one important technological parameter of the pastes was investigated—moisture content (%W). The moisture content of the pasted plates impacts the machine pasting and the following curing process [18]. The moisture content should be in the range of 8% to 11%, and for both pastes %W is into this range with 11.40% for CP and 11% for MVFP. This indicates that both pastes were prepared properly within the technological standards.

Table 3. Chemical analysis of the negative pastes before curing.

Sample	% Pb	% PbSO ₄	%PbO
CP	10.75	5.38	80.33
MVFP	9.45	9.61	77.62

Both negative pastes were once again subjected to chemical analysis after curing and the obtained results are presented in Table 4. The MVFP paste again has a higher content of PbSO₄ by 5.48%. The data in the table show that, after the curing process, the Pb content in both pastes is almost equal to around 6%, while the PbO content remains by 4.04% lower in the multivector field treated paste than in the control paste. In the course of the curing process, metallic lead oxidizes thus decrease their content in the cured paste. The data presented in Tables 3 and 4 indicate that both electrodes were cured under the same conditions and to the same degree.

Table 4. Chemical analysis of the negative pastes after curing.

Sample	% Pb	% PbSO ₄	%PbO
CP	6.91	7.18	80.78
MVFP	6.18	12.66	76.74

The X-ray diffraction method was used to determine the phase composition of the active masses of the two types of negative pastes (CP and MVFP) immediately after paste preparation and after curing. The samples were examined using an X-ray diffractometer “Philips” PW 1030, which has a θ – 2θ Bragg–Brentano geometry, with Cu K α radiation (30 kV, 20 mA), a wavelength $\lambda = 1.5406 \text{ \AA}$ and a scintillation detector. The output diffractograms were obtained at room temperature and at a constant scan rate and a reflection angle of 2θ in the range of $19 \div 40^\circ$ at a step of 0.02° . The obtained X-ray diffraction patterns were interpreted using the PCPDFWIN database, ICDD, 2002.

Figure 2a presents the XRD data of CP and Figure 2b presents the MVFP before curing. The XRD patterns feature higher intensity of α -PbO in the CP. The characteristic diffraction peaks of the tribasic lead sulfate (3BS) phases are of the same intensity in both pastes.

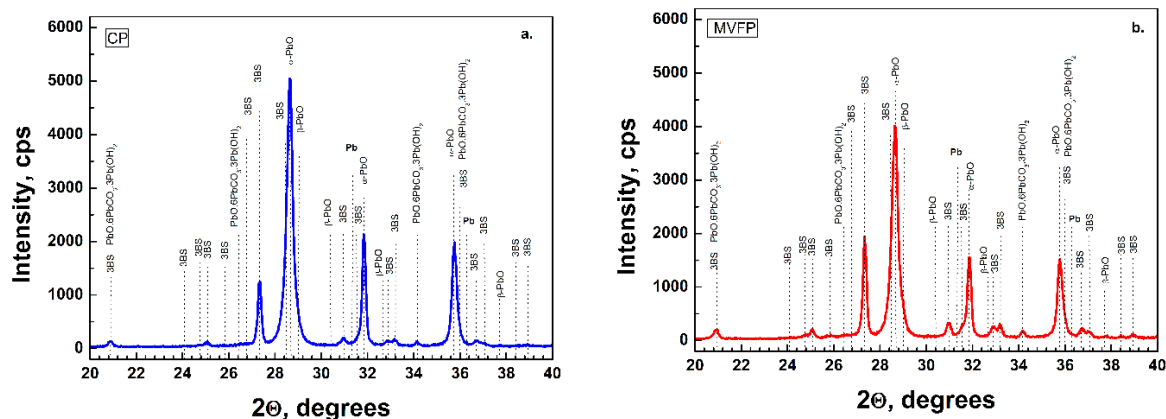


Figure 2. XRD analysis of control paste (a) and paste prepared with external application of multivector field (b) after mixing.

Figure 3 presents the results of the XRD analysis of CP and MVFP after curing. A very indicative effect of the application of the external multivector field is the change in intensity of α -PbO and 3BS. It can be seen that the intensities of α -PbO and 3BS diffraction peaks in MVFP are higher than in CP. As it was pointed out earlier, right after the paste mixing, the intensity of the XRD peaks of α -PbO was lower in the MVFP, but changed after the curing process. On the other hand, after curing, we observed higher 3BS intensity of MVFP compared to CP, while right after mixing, these peaks were of equivalent intensities. It can also be seen in Figure 3 that the XRD pattern of the CP features an intensity peak of $\text{PbO} \cdot 6\text{PbCO}_3 \cdot 3\text{Pb}(\text{OH})_2$ significantly higher than in the MVFP, despite the fact that both pastes were cured simultaneously in the same curing chamber under the same temperature and humidity conditions.

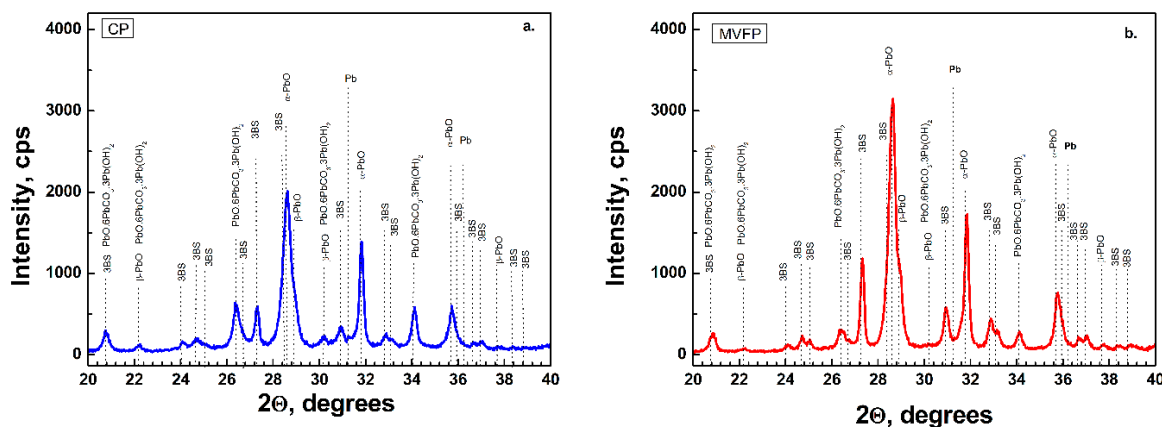


Figure 3. XRD analysis of control paste (a) and paste prepared with external application of multivector field (b) after curing.

For the purpose of the study, a phase analysis of the XRDs is performed using the Maud software [27] mainly based on the Rietveld method. The data are compared with the data of the volumetric titration. The results of these analyses are presented on Tables 5 and 6.

The comparison of the chemical composition estimates of negative pastes before curing is shown in Table 5 and after curing in Table 6. It should be noted that the NAM estimates for the amount of lead sulphate and lead monoxide identified by XRD are different from the one identified by volumetric titration. The reason is that these materials are in the form of very fine residual crystals that cannot reflect well the X-rays by XRD, or are surrounded by lead crystals that absorb X-rays and make their identification impossible by this method. In addition, the oxyhydrate groups are not visible by XRD. It should be noted that the sample preparation techniques for both methods are different, which may also lead to some differences.

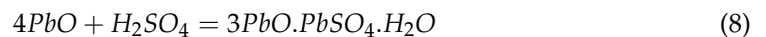
Table 5. Comparison of the chemical analysis by titration and XRD of the negative pastes before curing.

By Chemical Analysis							
	%Pb	% α -PbO	% β -PbO	%PbO	%PbSO ₄	%3BS	%PbO.6PbCO.3Pb(OH) ₂
CP	10.75			80.33	5.83		
MVFP	9.45			77.62	9.61		
By XRD (Figure 2)							
CP	0.045	80.12	0.072			18.25	1.50
MVFP	0.355	72.36	0.104			24.72	2.45

Table 6. Comparison of the chemical analysis by titration and XRD of the negative pastes after curing.

By Chemical Analysis							
	%Pb	% α -PbO	% β -PbO	%PbO	%PbSO ₄	%3BS	%PbO.6PbCO.3Pb(OH) ₂
CP	6.91			80.78	7.18		
MVFP	6.18			76.74	12.66		
By XRD (Figure 3)							
CP	0.32	42.33	0.83			44.84	11.58
MVFP	0.2	43.61	0.2			49.03	6.96

The main explanation for the difference in the data from chemical analysis by titration and XRD analysis is the 3BS, which is observed on the XRDs. The process of obtaining 3BS during paste mixing is well studied by Pavlov [18]. When the acid first contacts the wet PbO, it reacts to form lead sulfate (PbSO₄), which reacts with PbO to form basic lead sulfates. At temperatures below 71.1 °C, the stable basic sulfate is tribasic lead sulfate (3BS).



Formula (8) shows that 3BS is a complex composition of lead oxide, lead sulphate and water. Taking this into account, good correlation between the investigation methods is observed confirming all the above observations and conclusions.

In order to investigate the effects of the externally applied multivector field during paste preparation on the performance of lead cells, CP and MVFP pastes were used to prepare negative electrodes. Six 2 V/2.3 Ah cells were built with these electrodes and standard positive electrodes, at 50% utilization of the positive active mass. After curing, the cells were formed employing a formation protocol comprising eight steps and formation capacity equal to 3.5 times the theoretical capacity. After formation, the cells were cycled by C10 profile.

The capacity curves in Figure 4 show that the cells with negative electrode prepared with MVFP reached the theoretical nominal capacity of 2.32 Ah. The control CP cells exhibits an average initial capacity of 2.22 Ah, which is about 5% lower than that of the MVFP cells. During cycling, the cells with MVFP achieved, on average, 12% higher discharged capacity than the CP cells. On the last discharge cycle, the capacity of the CP cells averaged at 1.39 Ah, and for the MVFP cells, 1.65 Ah, which is a difference of approximately 20%. For all 10 cycles, the total discharged capacity was, on average, 16.52 Ah for CP cells and 18.36 Ah for MVFP cells. This is an average of 11% more total discharged capacity for MVFP than CP lead cells. The figure gives us grounds to conclude that the application of external multivector field during negative paste preparation influences the chemical reactions during paste preparation. It also influences the crystallization processes in the negative plates and, hence, the content and the structure of the negative active mass. It has a significant effect on the capacity of the prepared cells. This conjecture is also confirmed by the results of the chemical and XRD analysis of the pastes before and after curing.

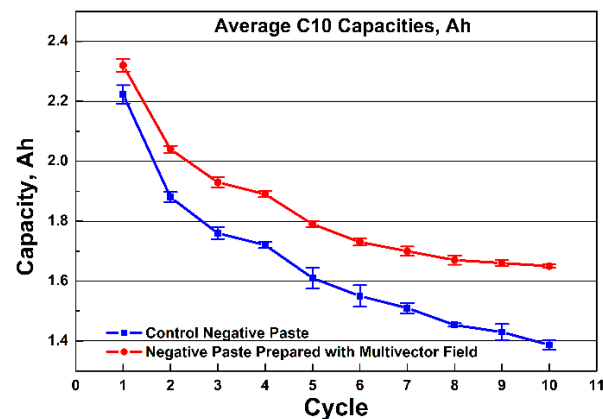


Figure 4. Averaged values from the 10 cycle C10 capacity measurements of the 6 cells with negative electrodes prepared with CP and MVFP.

3.2. Application of Multivector Field during Formation of Negative Electrodes

As was already explained above, two groups of 12 V/75 Ah batteries were formed for the purpose of this study. Two control batteries without application of multivector field during the formation—CB1 and CB2—and two batteries with application of multivector field during the formation process—MVFB1 and MVFB2. CB1 and MVFB1 were disassembled immediately after the formation for analysis of the negative electrodes, while CB2 and MVFB2 were cycled, employing a continuous 17.5% DoD test profile.

The results of the chemical analysis of CB1 and MVFB1 batteries are presented in Table 7. It can be seen that the content of Pb in MVFB1 is 2.14% less than in CB1, while the unconverted PbSO_4 in both batteries is the same, which suggests equal formation levels of the negative active masses in the two batteries. The obtained BET surface area values for the two types of negative active masses are $0.453 \text{ m}^2/\text{g}$ for CB1 and $0.43 \text{ m}^2/\text{g}$ for MVFB1, respectively. These results show that the specific surface in both negative active materials is almost the same. The XRD data presented in Figure 5 confirm the results from the chemical and BET analysis, namely, that both batteries were formed to the same formation level and the phase composition and structure of the negative active materials is preserved. It can be concluded that multivector field emission applied during formation of lead–acid batteries does not have an unfavorable effect on the negative active mass composition.

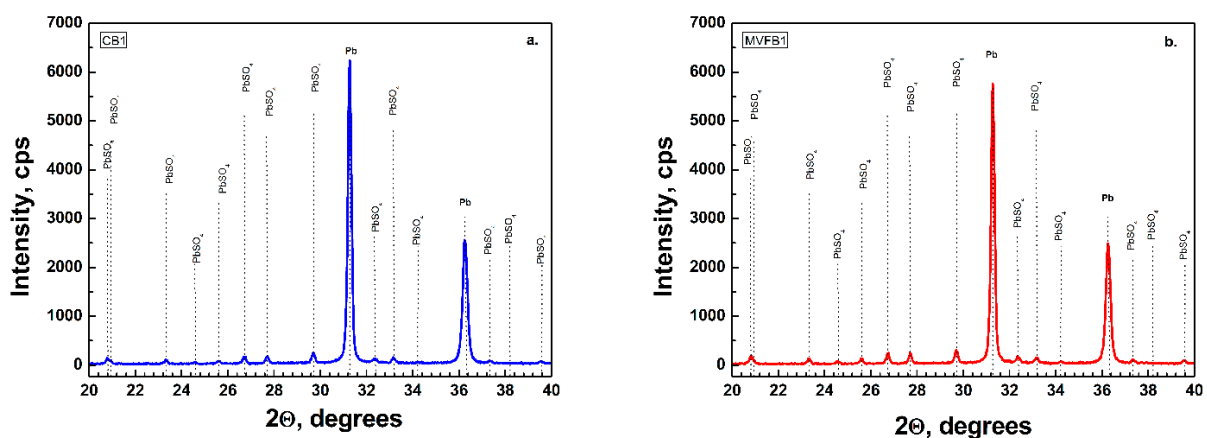


Figure 5. XRD analysis of control battery (a) and battery formed with external application of multivector field (b) after formation.

The XRD analysis gives us the opportunity to perform phase analysis of the chemical composition of the negative active material with the Maud software and compare it to the data of the chemical analysis by titration. This comparison is shown on Table 8.

Table 7. Chemical analysis of the negative active materials after formation.

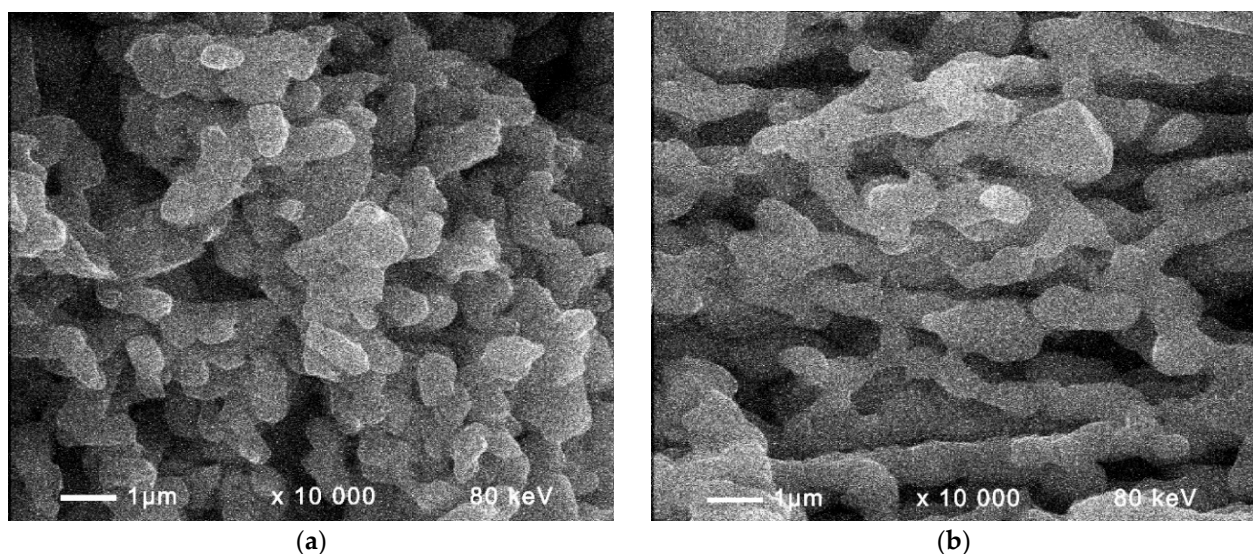
Sample	% Pb	% PbSO ₄	%PbO
CB1	89.18	6.86	2.34
MVFB1	87.04	6.79	4.38

Table 8. Comparison of the chemical analysis by titration and XRD of the negative active materials after formation.

By Chemical Analysis			
Sample	% Pb	% PbSO ₄	%PbO
CB1	89.18	6.86	2.34
MVFB1	87.04	6.79	4.38
By XRD (Figure 5)			
CB1	90.8	9.2	n.d.
MVFB1	86.66	13.34	n.d.

After formation of the NAM, we observed a good match in the percentage of lead, but due to the low content of PbO, on the XRD analysis, no characteristic peaks were observed and we cannot correctly calculate the content of oxides and sulfates. It should be noted that in the analytical methods used to determine the phase composition of the negative active masses in lead batteries, the relative error is not more than 0.2–0.4%. This value is confirmed by two parallel determinations of the same average sample.

Figure 6 shows SEM micrographs of negative active mass formed without external influence of the multivector field (Figure 6a) and with application of external multivector field (Figure 6b). The SEM image in Figure 6a features randomly distributed Pb particles, while the lead crystals in Figure 6b are interconnected in a network. In addition, a pronounced Pb skeleton can be seen in the SEM image of the negative active material formed under the influence of a multivector field (Figure 6b), which favors the subsequent efficient cycling.

**Figure 6.** SEM micrographs of the negative active mass of control battery CB1 (a) and battery formed with external influence of a multivector field MVFB2 (b) after formation.

After formation with and without the application of external multivector field, batteries MVFB2 and CB2 were subjected to initial C20 capacity tests. The batteries were

discharged with a current of 3.5 A down to a final voltage of 10.5 V. The recorded capacity of the CB2 battery was 74.36 Ah against 78.07 Ah for the MVFB2 battery. Both batteries reached a capacity close to their nominal capacity value of 75 Ah, but MVFB2 had a 4.75% higher initial capacity than CB2. After the initial capacity test, the batteries were charged for 24 h in a water bath at 27 °C, with a maximum current of 17.5 A and an upper voltage limit of 16 V. After that, the batteries were cycled at 17.5% DoD. At the end of each cycle, the final discharge voltage was recorded. The results of the 17.5% DoD test are displayed in Figure 7. It can be seen that the battery formed with the application of an external multivector field (MVFB2) had a higher final discharge voltage than the control battery (CB2). This is a clear indication of better charge retention in the battery, as well as better charge acceptance. Moreover, better stability of the discharge voltage of MVFB2 was observed. In the first third of the cycling test, the voltage of the control battery CB2 exhibited some instability, which might be due to the poorly formed Pb skeleton, as evident from the SEM micrographs. As was already mentioned earlier, a good Pb skeleton of NAM ensures more effective cycling of lead batteries. This statement is confirmed by the total number of cycles achieved by the two batteries. MVFB2 completed 352 cycles before it reached its end of life at 10 V, while CB2 reached 293 cycles. These results indicate a 20% longer cycle life for the battery formed with external influence by a multivector field. We may conclude that application of multivector field during formation of the negative active materials in lead–acid batteries has positive effect on the skeleton structure of the Pb crystals, and, hence, ensuring better cycle life performance.

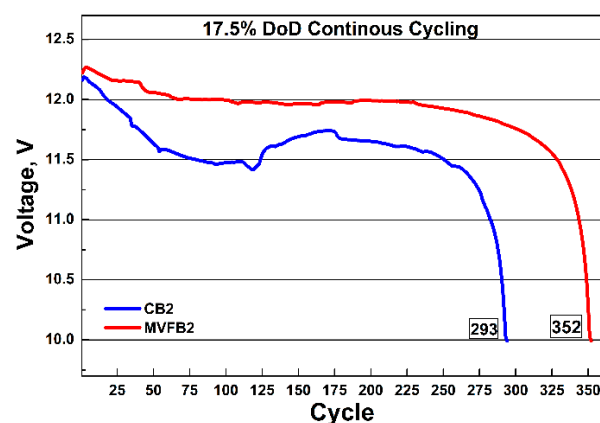


Figure 7. Final discharge voltages of control battery CB2 and battery formed with external influence of multivector field MVFB2 cycled at 17.5% DoD.

4. Theory

The most probable mechanism of influence of the multivector field on the chemical and electrochemical processes in lead batteries during negative paste preparation and formation of negative active masses is proposed.

It is known from the literature [10,28,29] that the result of chemical and electrochemical processes is the quantum rearrangement of the atomic nuclei of the chemical elements involved in the reactions and the rearrangement of their electron clouds in the formation of chemical compounds. It has also been found that the three fundamental elements of quantum mechanics are closely related and underlie the explanation of the mechanism of transformations described by electrochemical science. These three main factors are the following:

- The first factor is the electron wave function of the chemical elements, which describes the distribution of electrons in space and time, as well as the possible states of a physical system. The wave function of the electron also describes its spin.

- The second factor is the Pauli principle, which describes the distribution of electrons according to their energy level and spin state, i.e., (wave function), which creates the property ferromagnetism.
- The third element is the Schrödinger equation, which gives a quantum description based on classical mechanics. The solution of the Schrödinger equation includes the wave function ψ of a given quantum system at any point in space (x, y, z, t), called the quantum amplitude of probability. The square of the quantum amplitude makes it possible to determine the probability of a physical event at a given point in space.

These three factors of quantum mechanics are the basis of our attempt to explain the mechanism of the effects of the external multivector field on the chemical and electrochemical processes that occur in negative active masses for lead batteries during paste preparation and during formation of this electrochemical system.

The solution of the Schrödinger equation refers to the simplest chemical particles, such as a hydrogen atom consisting of a proton and an electron and it has the following form

$$H\Psi = E\Psi \quad (9)$$

where E is a constant equal to the energy level of the system and H is the Hamiltonian corresponding to the total energy of the system.

The solution of this equation determines the discrete value of the energy E and the wave function of the electron Ψ .

The above two equations represent the electron-proton chemical systems, which include only the Coulomb interaction forces and which determine the Coulomb potential of the respective electrochemical system.

Because the magnetic field has material properties and is a macro manifestation of the quantum micro properties of substances and magnetic fields affect the interactions between substances, which manifest as material objects with micro sized quantum characteristics. If we look at the chemical processes involved in the preparation of pastes and the complex scheme of the mechanism of the electrochemical processes of charge and discharge in lead–acid batteries, we shall see that magnetic fields change the weights of the substances involved, because in quantum interactions, the electronic properties of these substances change quantitatively. At the same time, protons are involved in the scheme of almost all chemical and electrochemical reactions. Therefore, for lead–acid electrochemical systems, which are composed of large amounts of electrons and atomic nuclei, the asymmetric wave function is valid, for which, according to Pauli's principle, the electrons of this system manifest as fermions characterized by a corresponding spin (i.e., own wave function). It is for this reason that the substances involved in the chemical and electrochemical reactions during the production of lead batteries and during their operation create the property of ferromagnetism. This is the main reason why the application of exposure to multivector field during paste preparation and formation of lead–acid systems strongly affects the wave function of the chemicals and reagents involved. In fact, due to the specific parameters of the applied multivector field, the wave function of the electrons and protons of the substances involved in the electrochemical reactions can change to a certain extent in a controlled manner. The change in the wave function creates a new physicochemical factor that can oscillate between the two spin states, the corresponding triplet state (non-reactive) and the singlet state (chemically active state) of the electrochemical system in a lead–acid cell. The result of this effect is a change in reactivity of the substances involved in the charge-discharge electrochemical processes or the formation of lead–acid batteries. These considerations and our attempts to describe the possible mechanism of the electrochemical processes in lead batteries gives us reason to offer the explanation that the application of external multivector field allows the transformation of the electrochemical reactions in lead batteries between the allowed and not allowed spin energy levels of the electrons from the substances involved in these processes. Thus, by applying a multivector field with defined parameters, conditions can be created allowing to control the reactivity of the different compounds that are involved in the various chemical and electrochemical processes. The

influence of the multivector field on the possibility of charge–discharge electrochemical processes in lead batteries can be represented by the following mathematical expression:

$$P = f[H, \alpha, \mu_n, I, H_I, \omega, J] \quad (10)$$

where H is the value of the magnetic field, α is the electron-nuclear Fermi-interaction, μ_n is the magnetic moment, I and m_i are the spin of the electron and the projection of the nucleus, H_I is the amplitude, ω is the frequency and J is the electron-nuclear magnetic interaction depending on the specific magnetic moment of the nucleus of any particular chemical element involved in the electrochemical reaction of charge, discharge or formation of active masses in lead batteries. The wave function, calculated in this way, determines the magnetic spin effects in the course of the electrochemical reactions and the possibilities for influencing the electrochemical processes of formation, current generation and current output in lead–acid batteries.

5. Conclusions

The chemical analysis of negative pastes for lead–acid batteries prepared with or without the application of external multivector field did not show significant differences in their chemical composition. The higher intensities of the 3BS and α -PbO peaks in the XRD pattern of the cured negative paste prepared with application of external multivector field signify better crystal structure and phase composition. These findings are confirmed by the capacity test results for lead–acid cells assembled with negative electrodes prepared with this paste. The cells with negative electrode prepared with paste under the influence of external multivector field exhibit on average 12% higher capacity than the control cells during 10 cycles C10 and average 20% more capacity on the last 10th cycle. This experimental finding gives us grounds to conclude that the chemical processes during the negative paste preparation under the influence of external multivector field proceed more efficiently, giving better phase composition and crystallinity of the cured paste, thus increasing steadily the capacity of the consequently built lead batteries.

Analysis of the chemical compositions of the negative active masses of batteries formed with and without the application of external multivector field show approximately the same values. Therefore, we can conclude that the external influence with the multivector field does not adversely affect the composition of the negative active mass during formation. Moreover, the SEM micrographs of these negative active masses show clearly that, in the negative active mass formed with influence of multivector field, the lead crystals are interconnected in a much better structured lead skeleton. The better lead skeleton after formation ensures better cycle life. In support of this conclusion are the results of the cycle life tests of the formed batteries, employing the 17.5% DoD cycling test. The battery formed with external influence of multivector field exhibits better voltage stability throughout the cycling test. In addition, the results of this test show that the battery formed under the influence of external multivector field completed 352 cycles until it reached its end of life at 10 V, while the lead–acid battery formed without multivector field reached 293 cycles, i.e., a 20% longer cycle life was achieved. We can conclude that the application of a multivector field during the formation of negative active materials in lead–acid batteries has a positive effect on the skeletal structure, size and shape of the Pb crystals, which ensures a longer service life of the batteries.

Based on these experimental results, a most probable mechanism of the influence of the multivector field on the chemical and electrochemical processes in lead batteries during negative paste preparation and the formation of negative active masses is proposed. The application of a multivector field can create conditions allowing control of the reactivity of the different compounds involved in the chemical and electrochemical processes. The calculated wave function determines the magnetic spin effects in the course of the electrochemical reactions and the possibilities for influencing the processes of formation, current generation and current output in lead–acid batteries.

Future works aim at investigating the effects of the multivector field on the positive paste preparation and positive active material formation. This will allow us to improve the most probable mechanism of the influence of the multivector field, thus enhancing the operational parameters of lead–acid batteries.

Author Contributions: Conceptualization, B.S., V.N. and U.M.; methodology, B.S. and V.N.; validation, B.S., V.N. and U.M.; formal analysis, B.S. and V.N.; investigation, B.S. and V.N.; resources, B.S., V.N. and U.M.; data curation, B.S. and V.N.; writing—original draft preparation, B.S.; writing—review and editing, V.N. and B.S.; visualization, B.S.; supervision, V.N.; project administration, B.S.; funding acquisition, B.S. and V.N. All authors have read and agreed to the published version of the manuscript.

Funding: This research has been partially financially supported by the project No BG05M20P001-1.002-0014 “Center of competence HITMOBIL—Technologies and systems for generation, storage and consumption of clean energy”, funded by Operational Program “Science and Education For Smart Growth” 2014–2020, co-funded by the EU from European Regional Development Fund.

Data Availability Statement: Not Applicable.

Acknowledgments: The authors acknowledge with thanks the technical assistance provided by Yovka Milusheva, Mariana Gerganska and Zhan Vasilev.

Conflicts of Interest: The authors declare no conflict of interest.

References

1. May, G.J.; Davidson, A.; Monahov, B. Lead batteries for utility energy storage: A review. *J. Energy Storage* **2018**, *15*, 145–157. [[CrossRef](#)]
2. Budde-Meiwes, H.; Schulte, D.; Kowal, J.; Sauer, D.U.; Hecke, R.; Karden, E. Dynamic charge acceptance of lead–acid batteries: Comparison of methods for conditioning and testing. *J. Power Source* **2012**, *207*, 30–36. [[CrossRef](#)]
3. Moseley, P.T.; Rand, D.A.J.; Davidson, A.; Monahov, B. Understanding the functions of carbon in the negative active-mass of the lead–acid battery: A review of progress. *J. Energy Storage* **2018**, *19*, 272–290. [[CrossRef](#)]
4. Foudia, M.; Matrakova, M.; Zerroual, L. Effect of a mineral additive on the electrical performances of the positive plate of lead acid battery. *J. Power Source* **2015**, *279*, 146–150. [[CrossRef](#)]
5. Pavlov, D.; Naidenov, V.; Milusheva, Y.; Vassilev, S.; Shibahara, T.; Tozuka, M. Benzyl benzoate as an inhibitor of the sulfation of negative electrodes in lead–acid batteries. *J. Energy Storage* **2018**, *17*, 336–344. [[CrossRef](#)]
6. Culpin, B.; Rand, D.A.J. Failure modes of lead/acid batteries. *J. Power Source* **1991**, *36*, 415–438. [[CrossRef](#)]
7. Wagner, R. Failure modes of valve-regulated lead/acid batteries in different applications. *J. Power Source* **1995**, *53*. [[CrossRef](#)]
8. Lam, L.T.; Haigh, N.P.; Phyland, C.G.; Urban, A.J. Failure mode of valve-regulated lead–acid batteries under high-rate partial-state-of-charge operation. *J. Power Source* **2004**, *133*, 126–134. [[CrossRef](#)]
9. Nakamura, K.; Shiomi, M.; Takahashi, K.; Tsubota, M. Failure modes of valve-regulated lead/acid batteries. *J. Power Source* **1996**, *59*, 153–157. [[CrossRef](#)]
10. Petrucci, R.H.; Herring, F.G.; Bissonnette, C.; Madura, J.D. *General Chemistry: Principles and Modern Applications*; Pearson: New York, NY, USA, 2017.
11. Naidenov, V.; Markov, U. Influence of ultrasonic waves on the formation of lead–acid batteries. *J. Power Source* **2012**, *217*, 236–242. [[CrossRef](#)]
12. Khare, N.; Singh, P.; Vassiliou, J.K. A novel magnetic field probing technique for determining state of health of sealed lead–acid batteries. *J. Power Source* **2012**, *218*, 462–473. [[CrossRef](#)]
13. Battaglia, V.; Newman, J. Magnetic Field Effects in High-Power Batteries: I. The Penetration of an Electric Field into a Cylindrical Conductor. *J. Electrochem. Soc.* **1994**, *141*, 703–708. [[CrossRef](#)]
14. Battaglia, V.; Newman, J. Magnetic Field Effects in High-Power Batteries: II. Time Constant of a Radial Circuit Terminated by a Cylindrical Cell with Inductance. *J. Electrochem. Soc.* **1994**, *141*, 708–713. [[CrossRef](#)]
15. Harrison, H.T.; Cooke, G.; Hewitt, D.A.; Stone, D.A.; Green, J.E. Magnetic tomography for lead acid batteries. *J. Energy Storage* **2017**, *12*, 1–10. [[CrossRef](#)]
16. Harrison, H.T.; Stone, D.A.; Green, J.E. Practical Current Distribution Measurement Systems for Lead Cells. *IEEE Trans. Instrum. Meas.* **2018**, *68*, 1–15. [[CrossRef](#)]
17. Barnes, S.C.; Matheison, R.T. The potential-pH diagram of lead in the presence of its implications in lead–acid battery studies. In *Batteries 2*; Elsevier: Amsterdam, The Netherlands, 1965; pp. 41–54.
18. Pavlov, D. *Lead–Acid Batteries: Science and Technology*, 2nd ed.; Elsevier: Amsterdam, The Netherlands, 2017.
19. Simon, A.C.; Jones, E.L. Crystallogenesis in the Forming of Plates for the Lead–Acid Storage Battery. *J. Electrochem. Soc.* **1962**, *109*, 760. [[CrossRef](#)]

20. Pavlov, D.; Iliev, V.; Papazov, G.; Bashtavelova, E. Formation Processes of the Lead–Acid Battery Negative Plates. *J. Electrochem. Soc.* **1974**, *121*, 854–860. [[CrossRef](#)]
21. Mateescu, A.; Vasloban, B.; Mateescu, C. The Effects of Using the Ultrasonic Waves and Current Impulses on Lead–acid batteries Forming Processes. In Proceedings of the TELESCON 1997—2nd International Telecommunications Energy Special Conference, Budapest, Hungary, 22–24 April 1997; pp. 357–362.
22. Markov, U. Method for Preparation of Positive and Negative Pastes for Lead–Acid Battery Cells and Batteries under the Influence of a Modulated Low-Energy Magnetic Field. Patent Number BG111931A, 30 September 2016.
23. Wang, J.; Dong, L.; Liu, M.; Wang, J.; Shao, Q.; Li, A.; Yan, W.; Jung, J.C.Y.; Zhang, J. Significantly improved high-rate partial-state-of-charge performance of lead–acid batteries induced by trace amount of graphene oxide nanosheets. *J. Energy Storage* **2020**, *29*, 101325. [[CrossRef](#)]
24. Pavlov, D.; Gancheva, S.; Andreev, P. Effect of hydrogen and oxygen on stability of expanders and performance of lead/acid batteries. *J. Power Source* **1993**, *46*, 349–359. [[CrossRef](#)]
25. Hu, J.; Wu, C.; Wang, X.; Guo, Y. Additives of suppressing hydrogen evolution at carbon-containing negative plates of valve-regulated lead–acid batteries. *Int. J. Electrochem. Sci.* **2016**, *11*, 1416–1433.
26. Jung, J.; Zhang, L.; Zhang, J. (Eds.) *Lead–Acid Battery Technologies*; CRC Press: Boca Raton, FL, USA, 2015.
27. Lutterotti, L.; Bortolotti, M.; Ischia, G.; Lonardelli, I.; Wenk, H.R. Rietveld texture analysis from diffraction images. *Z. Kristallogr. Cryst. Mater.* **2007**. [[CrossRef](#)]
28. O'Connor, C.J. Magnetochemistry—Advances in Theory and Experimentation. In *Progress in Inorganic Chemistry Book Series*; John Wiley and Sons: Hoboken, NJ, USA, 2007.
29. Hayashi, H. *Introduction to Dynamic Spin Chemistry*; World Scientific: Singapore, 2004.